# Ultra high energy $\nu_\tau$ detection with a cosmic ray tau neutrino telescope using fluorescence/Cerenkov light technique



2005 J. Phys. G: Nucl. Part. Phys. 31 571

(http://iopscience.iop.org/0954-3899/31/7/004)

INSTITUTE OF PHYSICS PUBLISHING JOURNAL OF PHYSICS G: NUCLEAR AND PARTICLE PHYSICS

J. Phys. G: Nucl. Part. Phys. **31** (2005) 571–582 doi:10.1088/0954-3899/31/7/004

# Ultra high energy $\nu_\tau$ detection with a cosmic ray tau neutrino telescope using fluorescence/Cerenkov light technique

**Z Cao**[1,2]**, M A Huang**[3]**, P Sokolsky**[2] **and Y Hu**[4]

[1] Institute of High Energy Physics, Beijing 100039, People's Republic of China
[2] High Energy Astrophys. Inst., University of Utah, Salt Lake City, UT 84112, USA
[3] General Education Center, National United University, Miaoli, 360, Taiwan, Republic of China
[4] University of Science and Technology of China, Hefei 230026, People's Republic of China

Received 20 November 2004
Published 21 April 2005
Online at stacks.iop.org/JPhysG/31/571

**Abstract**

We have investigated the possibility of $\nu_\tau$ detection using a cosmic ray tau neutrino telescope (CRTNT) based on air shower fluorescence/Cerenkov light detector techniques. This approach requires an interaction of a $\nu_\tau$ with material such as a mountain or the earth's crust. A $\tau$ lepton produced in the charged current interaction must escape from the earth and then decay and initiate a shower in the air. The probability for the conversion from $\nu_\tau$ to air shower has been calculated for an energy range from 1 PeV to 10 EeV. An air shower simulation programme has been developed using the simulation package Corsika. The trigger efficiency has been estimated for a CRTNT detector similar to the HiRes/Dice detector in the shadow of Mt Wheeler in Nevada, USA. A rate of about eight triggered events per year is expected for the AGN neutrino source model with an optimized configuration and duty cycle of the detector.

(Some figures in this article are in colour only in the electronic version)

## 1. Introduction

The source of cosmic rays with particle energies above $10^{15}$ eV (1 PeV) remains unknown. A point source search could be a useful approach for solving this puzzle. Searches for point sources are best performed using observations of neutral particles because they can be directly traced back to the source. The universe is opaque to photons above $10^{14}$ eV due to interaction with the 2.7 K cosmological microwave background. The neutrino is another type of neutral particle that can be used to explore cosmic ray sources in this energy region. Newly discovered evidence of neutrino oscillation [1] leads to a plausible argument that the astrophysics neutrino flux will have an even flavour ratio of $\nu_e : \nu_\mu : \nu_\tau = 1 : 1 : 1$ [2].

One obvious effect of neutrino mixing is the appearance of tau leptons. This opens a window for cosmic ray source searches using air shower techniques since the decay products of $\tau$ leptons, mainly hadrons and electrons, will induce a detectable shower in the air.

Neutrinos convert into electrons, muons and taus through the charged current interaction. The interaction probability is much higher in the earth than in the atmosphere, due to the higher density of rock. However, electrons will shower quickly inside the target material. Muons travel very long distances before they decay but can only be detected by the small energy loss along the trajectory. A large detector, such as IceCube, buried inside the target material, is designed to detect those muons (track-like signals) and electrons (shower-like signals), but is inefficient for tau detection. At energies below 1 PeV, the tau decays and initiates a shower that cannot be distinguished from an electron shower. Between 1 and 20 PeV, a 1 km$^3$ size under-ice/water detector can clearly see the tau leptons by the so-called double-bang signature, with one shower from hadronic fragments of target nucleon in the neutrino–nucleon charged current interaction and one shower from the decay of the tau lepton. At energies above 20 PeV, the tau decay distance is longer than the width of 1 km$^3$ size detector and only one of the double bang showers can be seen. At higher energies, the neutrino flux is much lower and a 1 km$^3$ size detector is not large enough to detect such a flux.

One way to avoid constraints from the target volume is to separate the detection volume from the target volume. A fluorescence light detector such as HiRes or a Cerenkov light detector such as Dice has proven to be a successful detector with a small physical size but a huge detection volume. Leptons produced via charged current interactions must be able to escape from the target volume, decay in the atmosphere and develop a shower before they reach the detector for this scheme to work. Since the earth becomes essentially opaque to neutrinos at energies higher than 1 PeV, only neutrinos with paths close to and nearly parallel to the earth's surface, i.e. close to horizontal, are observable. These are known as *earth-skimming neutrinos* [3, 4]. The conversion efficiency from a tau neutrino to a tau is approximately $R_d\rho/\Lambda_I$, where $\rho$ is target density. $R_d$ is range of the tau in the target and $\Lambda_I$ is the neutrino charged current interaction length in grams per square cm in the target [5]. At energies above 1 PeV, tau leptons have a range such that the conversion probability in the earth is higher than that in the atmosphere [6]. The conversion efficiency becomes much higher at higher energy because $R_d$ increases less than linearly with energy, but $\Lambda_I$ decreases proportional to $E^{-0.36}$ [7]. This unique mechanism of detecting $\tau$-neutrinos provides an acceptance that is much larger than 1 km$^3$ underwater/under-ice detector arrays, especially at energies higher than 10 PeV. Detecting the tau lepton from earth-skimming neutrinos becomes an excellent way to study ultra high energy neutrino astronomy and to provide a possible proof of neutrino flavour oscillation.

The rest of the paper is organized as follows. In section 2, the conversion from tau neutrino to air shower and possible shower detection are discussed. The CRTNT detector is proposed at a potential site. A simulation of $\nu_\tau$ to $\tau$ conversion, shower development and shower detection are described in section 3 in detail. The event rate and its optimization are presented in section 4. Final conclusions are summarized in the last section.

## 2. Feasibility study

We first try to evaluate the detection of tau neutrinos skimming through mountains, then discuss the detection techniques and a potential site for the proposed CRTNT project.

### *2.1. $\nu_\tau$ to air shower conversion*

Two coordinate systems are used in this study. A three-dimensional local coordinate system describes the detector position and local topological information. The other is a

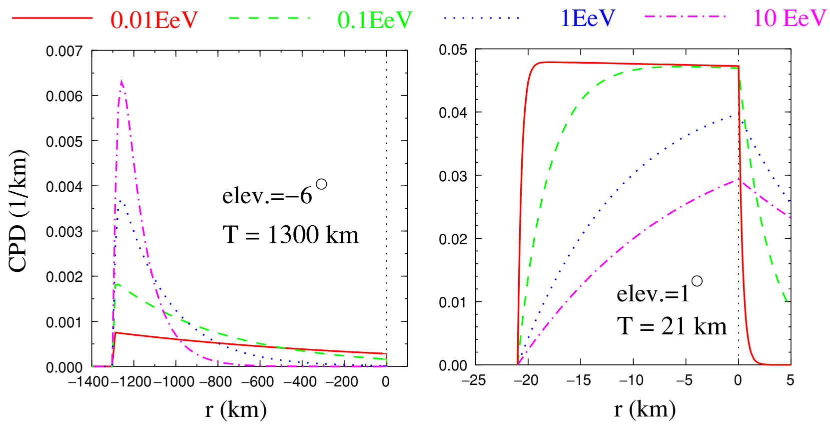


**Figure 1.** $\nu_\tau$ to shower conversion probability density (CPD) as a function of distance along trajectory.

one-dimensional coordinate system along the neutrino trajectory used for describing the mountain-passing/earth-skimming process.

The trajectory is described by the elevation angle $\epsilon$, the azimuth angle $\phi$, and the location of the escape point from the mountain/earth surface $(x_e, y_e, z_e)$ in the 3D local coordinate system. In the 1D coordinate system, $\nu_\tau$ travel from negative infinity and enter the mountain at $r = -T$, where $T$ is the thickness of the mountain or the earth's crust. The density distribution $\rho(r)$, and the total path length $T$ are different depending on the geometry of the trajectory. The incident $\nu_\tau$ interacts between $-T$ and 0, the $\tau$ then decays and initiates a shower at $r$. The probability of such a conversion from $\nu_\tau$ to a shower is a convolution of interaction probability of $\nu_\tau$ before distance $r$ and the probability of decay to a shower at $r$. It simplifies to

$$p_c(r;T)\,\mathrm{d}r = \begin{cases} \frac{1}{1-\mathrm{e}^{-T\rho/\Lambda}}\frac{\mathrm{d}r}{R_d-\Lambda_I/\rho}\left[\mathrm{e}^{-\frac{r+T}{R_d}} - \mathrm{e}^{-\frac{r+T}{\Lambda_I/\rho}}\right] & (-T < r < 0) \\ \frac{1}{1-\mathrm{e}^{-T\rho/\Lambda}}\frac{\mathrm{d}r}{R_d-\Lambda_I/\rho}\left[\mathrm{e}^{-\frac{T}{R_d}} - \mathrm{e}^{-\frac{T}{\Lambda_I/\rho}}\right]\mathrm{e}^{-\frac{r}{R_d}} & (r \geqslant 0) \end{cases} \quad (1)$$

where $p_c(r;T)$ is the conversion probability density (CPD) for a given trajectory $T = T(\epsilon, \phi, x_e, y_e)$, $\Lambda_I$ is the $\nu_\tau$ charge current interaction length in g cm$^{-2}$ and $R_d$ is the average range of $\tau$ lepton in km, i.e. $R_d = f\gamma c\tau$ where $\gamma$ is the Lorentz boost factor, $\tau$ is the lifetime of the $\tau$ lepton and $f$ is a fraction accounting for the energy loss [8]. $f$ decreases from 0.8 at $E_\tau = 100$ PeV to 0.2 at $E_\tau = 1$ EeV [5]. Figure 1 shows two cases of the CPD as functions of $r$ corresponding to down-going ($\epsilon > 0$, through a mountain about 21 km thick) and up-going earth-skimming ($\epsilon < 0$, through the earth's crust about 1300 km thick) trajectories.

As shown in figure 1, for energies lower than 10 PeV, the CPD is flat because of the long interaction length of the $\nu_\tau$ and the short decay length of the $\tau$ lepton. Only primary $\nu_\tau$ that interact close to the surface can produce an observable $\tau$. For $E_\nu$ above 10 PeV, the CPD peaks around 10–20 km in thickness of rock. The energy loss in the target material reduces both the survival rate and the energy of $\tau$ above $10^{17}$ eV. These results are consistent with other recent calculations [4, 5].

### *2.2. Detection of earth skimming $\nu_\tau$*

The $\tau$ lepton flux induced by an earth-skimming neutrino flux will be orders of magnitude lower than the cosmic ray flux in the observational window, a range from 1 PeV to 10 EeV [9].

A successful detection would require a detector having a large acceptance, of the order of several $km^2$ sr to over 100 $km^2$ sr. Because most earth-skimming neutrinos are concentrated near the horizon, the detector should have a great sensitivity to horizontal showers. Ground detector arrays have small trigger efficiency for both upward and downward going showers in the vicinity of the horizontal direction and hence cannot be very efficient for detecting $\nu_\tau$. Detection through optical signals would seem to be more efficient. A combination of fluorescence light and Cerenkov light detector in the shadow of a steep cliff could achieve this goal.

A fluorescence light detector, such as the HiRes prototype experiment [10], has a large FOV and acceptance. The difficulty is that it has to be operated at a high threshold corresponding to above 0.3 EeV, because of noise from sky background light. Cerenkov radiation provides many more photons along the shower axis. It can be useful for lowering the detection threshold. The Dice experiment [11] successfully measured the energy spectrum and composition of cosmic rays between 0.1 PeV and 10 PeV using the same detector but triggered by Cerenkov light. To maintain a good energy resolution, a typical Cerenkov telescope has to be operated within a small FOV of about a few degrees with respect to the air shower since the Cerenkov light intensity is a rapidly decreasing function of the viewing angle. On the other hand, a fluorescence light detector has to be operated with large viewing angle to the shower axis to avoid significant Cerenkov light contamination that can cause poor shower energy resolution. In order to achieve satisfactory statistics for the neutrino flux measurement, we have to lower the threshold while maintaining a large aperture.

Several points need to be stressed. First of all, the shower energy resolution is not crucial for neutrino searches, hence the Cerenkov light can be tolerated and can be useful for triggering the detector. Secondly, sky noise can be suppressed by placing the detector in the shadow of a mountain. A steep mountain in front of the detector is shown to be a good target for neutrino conversion in the above discussion. It also serves as a screen to block sky noise. Because of the low light background, the detector can be operated with a lower threshold as a fluorescence light detector. More importantly, the background from cosmic rays at the same or lower energies is much reduced. This makes the $\nu_\tau$ events distinguishable from the cosmic ray events. Finally, to enlarge the FOV of the detector, the telescopes can be configured to surround the mountain and minimize overlaps between telescopes.

In order to obtain sufficient fluorescence and Cerenkov light, we have to have a sufficient space for air shower development. A steep mountain side provides a large elevation coverage for the detector and a large open space between the mountain surface and the detector. An ideal site for observations would be a steep mountain, and a dry and clear atmospheric environment is essential for the fluorescence/Cerenkov light techniques.

In this paper, we consider placing the CRTNT detector in proximity to Mt Wheeler Peak (3984 m a.s.l.) near the Nevada–Utah border, USA. The mountain lies in a north-south direction and is about 40 km long. The west side is very steep. Further west, there is a flat valley about 30 km wide at about 1500 m a.s.l. For a detector located about 12 km away from the peak horizontally, the shadow of the mountain is about $11.7^\circ$ in elevation. It almost completely blocks the FOV of the telescopes of the CRTNT detectors proposed below. Within the shadow, the sky noise background should be less than that from the open sky. At Dugway, Utah, about 120 km north of the Wheeler Peak, the light background was measured to be 40 photon $\mu s^{-1}$ $m^{-2}$. In this paper, the light background for all the telescopes in the shadow is assumed to be the same as at Dugway. This is the upper limit to the sky noise. An on-site measurement for the actual background light will be done using a prototype detector.

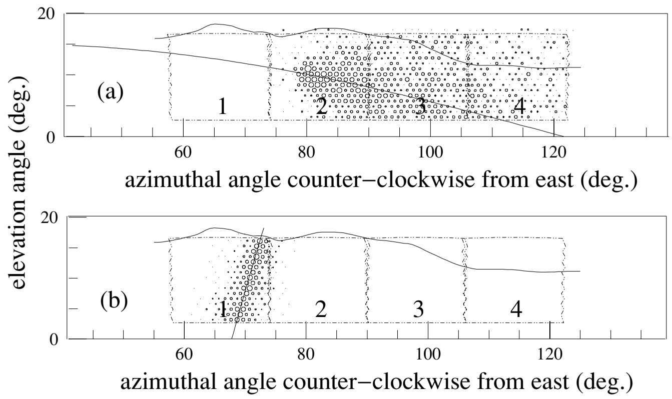


**Figure 2.** Simulated air showers seen by the CRTNT detector. (a) A $\tau$ neutrino-induced air shower starting and developing completely in the shadow of the mountain. The line along the shower direction represents a plane which contains the detector and the shower axis. The dashed lines show the boundary of the field of view of each telescope. The thick solid curve represents the profile of the Mt Wheeler Peak. Circles represent triggered tubes, and the size of each circle is proportional to the logarithm of the number of photons seen by the tube. (b) A normal cosmic ray air shower event coming down and hitting the slope of the mountain.

### *2.3. The CRTNT fluorescence/Cerenkov light detector*

The proposed CRTNT project uses fluorescence/Cerenkov light telescopes analogous to the detectors of the HiRes and the Dice experiments [19]. The telescopes are distributed in three groups located at three sites separated by eight km in the valley facing the west side of Mt Wheeler Peak. At each site, four telescopes observe an area of the mountain with 64° in azimuth and 14° in elevation. This area is about 14 km long in the north-south direction. The total field of view covers about $60^\circ \times 14^\circ$ and 70 km$^2$ with small overlaps between the telescopes on the three sites.

A 5.0 m$^2$ light collecting mirror with an reflectivity of 82% is used for each telescope. The focal plane camera is made of $16\times 16$ pixels. Each pixel is a 44 mm hexagonal photomultiplier tube that has about a $1^\circ \times 1^\circ$ field of view. Each tube is read out by a 50 MHz flash ADC electronics system to measure the waveform of the shower signals.

A pulse area finding algorithm is developed for providing an individual channel trigger using a field programmable gate array (FPGA). The first level trigger is set by requiring the signal–noise ratio to be greater than $4\sigma$, where $\sigma$ is the standard deviation of the total photo-electron noise during the signal pulse. The noise level is different for each pulse because the pulse duration varies depending on the distance to the light source. The second level trigger requires at least five channels triggered within a $5\times 5$ running subcluster over a single telescope camera of $16\times 16$ pixels. The trigger condition for an event is that at least one telescope is triggered. All triggers are formed by FPGA chips. Event data from all channels are scanned with a threshold lower than the trigger threshold from the FPGA buffers into a local Linux box.

A Monte Carlo simulation programme for the detector is developed as described in the next section. Thousands of showers initiated by the products of $\tau$-decays and normal cosmic rays are generated. The rest of this paper is based on this simulation. Two simulated event examples are shown in figure 2. In figure 2(a), a $\tau$ neutrino-induced air shower starts in the shadow of the mountain where a normal cosmic ray event is not expected. By contrast, a

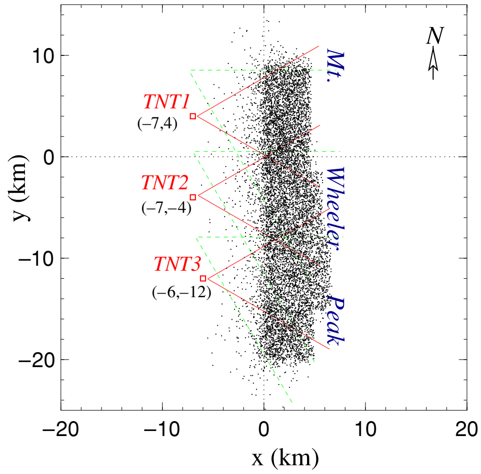


**Figure 3.** Locations of starting points of showers induced by $\tau$ neutrinos through Mt. Wheeler Peak near the Utah/Nevada border. The squares represent CRTNT telescopes. The solid lines attached to the detectors indicate the FOV of the telescopes. The dashed lines show a further optimization for detecting $\nu_\tau$ from the centre of our galaxy (see text in section 5 for details).

normal cosmic ray event is shown in figure 2(b). Figure 3 shows the detector configuration and shower initial point locations.

## 3. Monte Carlo simulation

In the simulation, the incident $\nu_\tau$ is coming from an interval of elevation angles between $-11^\circ$ and $17^\circ$, where the negative direction means a upward-going neutrino. The azimuth range is from $90^\circ$ to $270^\circ$, with all directions from the back of the mountain (the $x$-axis is pointing to the east). The flux of neutrinos is assumed to be isotropic and uniform in the field of view of the detector. Every incident $\nu_\tau$ is tested to see if it interacts inside the rock. If the neutrino interacted, the energy and momentum of the produced $\tau$ are calculated up to its decay point. The energy loss and the range of the $\tau$ lepton are calculated according to the result of [8]. If the $\tau$ decays outside the rock, there is about an 80% probability that an electron or multiple hadrons, mainly pions or kaons, are produced in the decay. These particles will initiate electromagnetic or hadronic showers from the decay point. The shower type and energy are determined by a standard $\tau$ decay routine and passed to an air shower generator. However, if the $\tau$ flies too far from the mountain surface before its decay, showers could be initiated behind the detector and would not be detected. In the simulation, $\tau$ that decay anywhere further than 7 km from the escape point on the mountain surface are ignored.

On the other hand, if the $\tau$ decays inside the rock, a regeneration procedure will be started in the simulation. This procedure repeats the previous process using the decay-product $\nu_\tau$ whose energy is determined by the same $\tau$-decay routine mentioned previously. Since the energy reduction in the $\nu_\tau$ to electron/hadron conversion is rather large, there is no need to repeat this regeneration procedure in further decays because the shower energy is lower than the threshold of the detector. The regenerated $\tau$ which decay inside the rock again are ignored.

### *3.1. From tau neutrino to tau lepton*

The $\nu_\tau$ to shower conversion efficiency is defined as the ratio between the total number of successfully converted events and the number of incident $\nu_\tau$. The simulation yields the conversion efficiency of $1.99 \times 10^{-4}$ and $2.21 \times 10^{-2}$ for the AGN [12] and GZK [16] neutrino source models, respectively. A distribution of locations where showers start developing is shown in figure 3. The detectors and their fields of view are shown in the same figure. The distributions of trigger efficiency as a function of energy are shown in figures 6 and 5. The conversion probability is different for different models mainly because the GZK neutrino energy spectrum is much harder than the AGN's, therefore they have a different pile-up effect associated with $\tau$ energy loss.

Because of the rather strong energy loss of the $\tau$ through ionization and radiation, the energy of the re-converted shower via $\nu$-regeneration is significantly lower. The contribution from the $\nu_\tau$-regeneration to the final detectable shower event rate is not significant. The regenerated $\nu_\tau$-shower conversion efficiency is less than 0.6% and 2.0% of the total conversion efficiency for AGN and GZK neutrinos, respectively.

### *3.2. Air shower simulation*

Corsika 6.0 [17] is used to generate air showers in the space between shower initiating point outside the mountain and the CRTNT telescopes. Because the detector is located about 12 km away from the mountain peak horizontally, the typical distance available for shower development is about 10 km in the air. Since all showers are initiated in an almost horizontal direction, the air density along the path of the shower development is nearly constant. Thus a uniform air density is assumed for the air shower development. A simulated shower library is established by generating 200 hadronic and 200 electromagnetic showers at three values of $1\times$, $2\times$ and $5\times$ the energies of each order of magnitude between 10 PeV and 1 EeV. The shower longitudinal profiles, i.e. number of charged shower particles along the shower axis, are stored in the library at every 5 g cm$^{-2}$.

Once a $\tau$ decays outside the mountain surface, it starts an air shower unless the decay product is a $\mu$. The decay point is taken as depth zero g cm$^{-2}$ for the shower development. A shower profile is randomly selected from the library in the group of showers at the closest energy. A number of charged particles of this shower are scaled up or down to represent the shower to be simulated. The amount of scaling is determined by the difference between the given shower energy and the energy of the selected shower. Some shower examples are shown in figure 4. Note that the longitudinal development behaviour is quite different from that of showers that develop from the top of the atmosphere to the ground where the density of the air increases nearly exponentially. Moreover, the hadronic showers develop noticeably faster than electromagnetic showers.

### *3.3. Photon production and light propagation*

Charged shower particles excite the nitrogen molecules as they pass through the atmosphere. The deexcitation of the molecules generates ultra-violet fluorescence light. The number of fluorescence photons is proportional to the shower size, and these photons are emitted isotropically. The shower simulation carried out in this paper assumes a fluorescence light spectrum according to a recent summary of world-wide measurements [18], including the dependence of the yield on the atmospheric pressure and temperature.

Since energies of charged shower particles are higher than the critical energy, the shower particles generate Cerenkov photons at every stage of the shower development. The accumulated Cerenkov light is concentrated in a small forward cone, therefore the intensity of the light is much stronger than the fluorescence light along the shower direction. Even for low energy showers at 500 TeV, the strong forward Cerenkov light beam can be detected if the shower points directly towards the detector. For showers coming from other directions, a

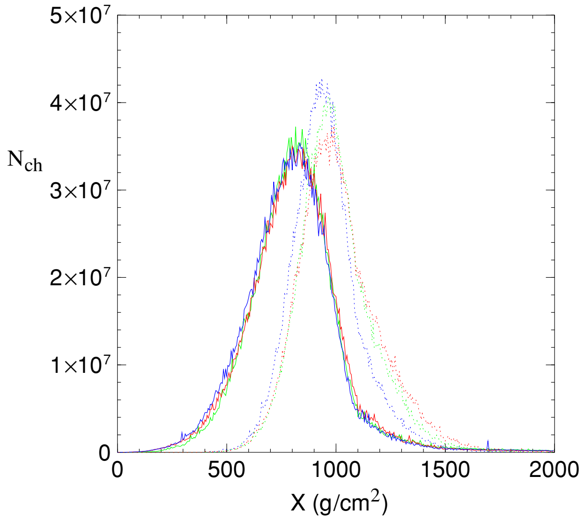


**Figure 4.** Showers generated by Corsika at energy $5\times10^{16}$ eV. Solid lines are hadronic showers. Dotted lines are electron showers.

significant part of the Cerenkov light is scattered out via Rayleigh and Mie scattering during the whole shower development history. The fraction of this light scattered in the direction of the detector can also make a noticeable contribution to detector triggering.

Cerenkov light generation and scattering is fully simulated. A detailed description of the calculation can be found in [19] and references therein.

Shower charged particles and therefore fluorescence light photons, spread out laterally following the NKG distribution function. The Moliere radius parameter of the NKG function is about 95 m at about 1500 m a.s.l. Photons originating from Cerenkov radiation have an exponential lateral distribution from the axis of the shower. Therefore, photons coming from a shower are spread over a range of directions around the shower location in the sky due to its longitudinal motion and lateral extension. A ray tracing procedure is carried out to follow each photon to the photo-cathode of PMTs once the photon source is located in the sky. All detector responses are considered in the ray tracing procedure, including mirror reflectivity, UV filter transmission, quantum efficiency of photo-cathode, location-sensitive response function of the photo-cathode and optical effects associated with the off-axial and defocusing effects. The technical parameters of the detector are set to be the same as the existing HiRes detector. More details on the detector specifications can be found elsewhere [19]. Sky noise photons are randomly added in this ray tracing procedure both in time and arrival directions.

The uncertainty associated with the varying weather conditions is negligible for the Rayleigh scattering. Scattering due to aerosols is more dependent on weather conditions. However, for a detector that has an aperture within 6 km, the aerosol scattering contribution to light extinction is close to minimum. The uncertainty in the triggering efficiency due to weather conditions is thus small. In the simulation, an average model [20] of aerosol scattering for western US deserts is employed.

## 4. Predicted event rate

For the CRTNT detector, we calculate the event rate using the $\nu_\tau$ to air shower conversion algorithm and the shower/detector simulation described above. Since the primary neutrino

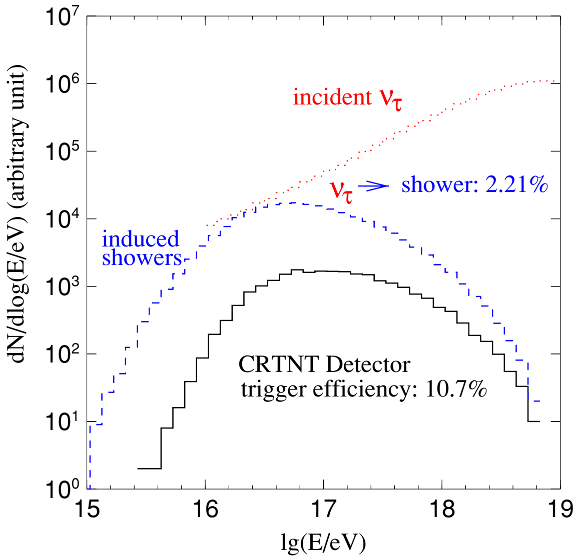


**Figure 5.** GZK $\nu_\tau$ to air shower conversion and triggering rate. The incident $\nu_\tau$ energy spectrum (dotted line) and converted shower energy distribution (dashed line) are plotted. The triggered air shower event distribution (solid) is calculated based on a detector described in section 2.3 and an air shower development algorithm described in section 3.2.

energy spectra are different in different production models, induced air showers from different sources have a slightly different detection efficiency. In order to illustrate the difference, two extreme cases are simulated in this paper. For a model dominated by low energy neutrinos (still above the threshold of the CRTNT detector), we use the AGN neutrino source model [12]. For a model with many more higher energy neutrinos, we use the GZK neutrino source model [16]. We generate $10^9$ and $10^7$ trials for AGN and GZK models, respectively.

Due to the stronger energy loss of the higher energy $\tau$ leptons, the observed GZK neutrino spectrum is severely distorted. The high energy neutrinos pile up at low energies once they are converted into lower energy showers. On the other hand, the shower-triggering simulation shows that the trigger efficiency is slightly higher for higher energy showers. The competition between those two effects yields a relatively flat event rate distribution between 10 PeV and 2 EeV. The distribution is shown in figure 5. The overall detection efficiency is $2.4\times10^{-3}$. Using the flux suggested by authors of [16] and a typical 10% duty cycle of the fluorescence/Cerenkov light detector, the event rate is about $0.23 \pm 0.01$ per year.

The predicted AGN neutrino flux in [21] is ruled out by the AMANDA experiment [22]. In this paper, we use an updated prediction of the AGN neutrino spectrum [12]. The source spectrum changes from $\sim E^{-1}$ to $\sim E^{-3}$ near 10 PeV. The neutrino flux is cut off around 0.6 EeV. In this case, the energy loss of the $\tau$ lepton inside the mountain is no longer significant. The converted shower spectrum has a similar shape to the incident neutrino spectrum at high energies. The conversion efficiency drops rapidly with energy in the low energy region. This softens the event rate as a function of energy below 10 PeV.

The average trigger efficiency of showers induced by the products of $\tau$-decays is 11.0%. The overall detection efficiency of AGN neutrinos is $2.19 \times 10^{-5}$. The spectra of $\nu_\tau$ are shown in figure 6. Using the flux predicted by the authors of [12], the event rate is found to be $5.04 \pm 0.05$ per year, where a 10% duty cycle is assumed for the detector.

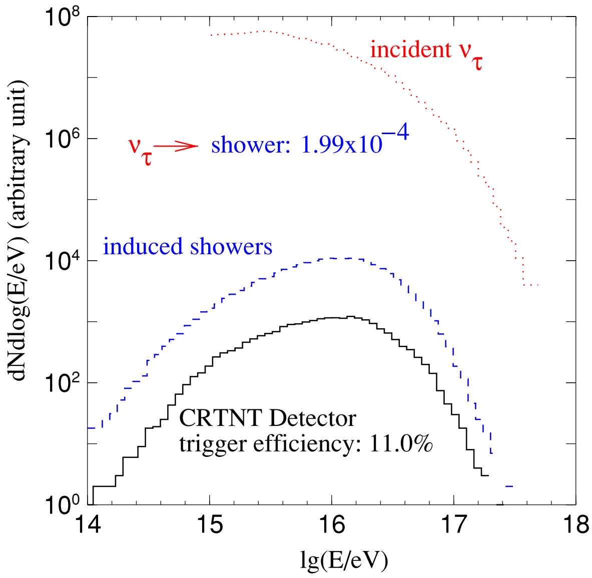


**Figure 6.** AGN $\nu_\tau$ to air shower conversion and triggering rate. The incident $\nu_\tau$ energy spectrum (dotted line) and converted shower energy distribution (dashed line) are plotted. The triggered air shower event distribution (solid) is calculated according to a detector described in section 2.3 and an air shower development algorithm described in section 3.2.

### *4.1. Optimization*

Using the simulation tool, we have tried to optimize the configuration of the detector to maximize the event rate. We find that the distances between the telescopes and the mountain are important parameters. Without losing much of the shadow size, the detection efficiency is higher if the telescopes are placed further from the mountain up to a distance of about 12 km. For the site near Mt Wheeler Peak, the altitude of the detectors is about 1500 m a.s.l. at 12 km from the mountain. This yields a shadow of about 11.7° on the detector. A single layer detector configuration shown in figure 2 maximizes the trigger efficiency of the neutrino detection. Using an array configuration of three single layer detectors separated by 8 km (see figure 3) maximizes the usage of the mountain body as a $\nu_\tau$ to shower converter.

Since the detector has a limited field of view towards the east, more than 3/4 of the field of view of the telescope is covered by the mountain shadow. The moon will not be in the field of view most nights. The level of moon light scattered towards the detector will be sufficiently low when the moon moves behind the telescopes. The detector should be able to be operated under such conditions. Conservatively, the useful observation time can then be increased by 50%. A rate of about eight events per year could then be expected for the AGN model case. More accurate estimation requires an on-site measurement for the light background with the moon up.

In this paper, $\nu_e$ and $\nu_\mu$ are not taken into account. From the point of view of the $\tau$ neutrino search, showers induced by these neutrinos are the background. However, for the purpose of particle astronomy, these neutrinos carry the same information about the source as the $\nu_\tau$ does. Since the $\mu$ generated in $\nu_\mu + A$ interaction hardly ever interacts and does not initiate a shower in the air, there is nearly no chance for it to trigger the detector. However, both $\nu_e$ and $\nu_\mu$ transfer 20% to 30% of energy to the target in the deep inelastic scattering (DIS) processes. The fragments of the target particles can induce detectable showers in the air if the neutrinos interact in a very thin layer of rock right beneath the surface. The contribution of the DIS processes could be enhanced because the neutral current processes also contribute to the detectable air shower generation. $\sigma_{\rm CC} + \sigma_{\rm NC}$ is the effective DIS cross section, in which the neutral current cross section $\sigma_{\rm NC}$ is about 44% of the charged current cross section $\sigma_{\rm CC}$ at $10^{15}$ eV and 31% at $10^{20}$ eV [7]. The interaction length for these processes is still very long, e.g. $6.6 \times 10^8$ g cm$^{-2}$ for $10^{16}$ eV and $2.2 \times 10^7$ g cm$^{-2}$ for $10^{20}$ eV. Since the total thickness of the mountain is about 20 km, i.e. $5.2 \times 10^6$ g cm$^{-2}$, we can assume the free paths of neutrinos to be a uniform distribution. Assuming that only DISs which happened within a layer of one to two radiation lengths behind the mountain surface are able to generate detectable showers, the DIS event conversion efficiency is approximately $5 \times 10^{-6}$. Comparing to the $\nu_\tau$-shower conversion efficiency of approximately $3 \times 10^{-4}$ at $10^{16}$ eV, the ratio of DIS events versus $\nu_\tau$ events is only about 1.7%.

For higher energies, the mean free path of the neutrino is shorter but only by one order of magnitude over three decades of energies. Thus the flat free path distribution is still a good approximation. The $\nu_\tau$-shower conversion efficiency increases with energy rather rapidly. The ratio between number of DIS events and number of $\nu_\tau$ events reduces to 0.04% at $10^{19}$ eV.

## 5. Conclusion

The technique of using a mountain to convert $10^{16}$–$10^{19}$ eV neutrinos to air showers and using fluorescence/Cerenkov light to detect the showers can be optimized by setting the detector near a $\sim 20$ km thick mountain body. Mt Wheeler near the Nevada/Utah border is a good example of maximizing the conversion in this energy range. The energy reduction in the conversion process is so severe for high energy $\tau$ that showers pile up below $10^{17}$ eV in the shower energy spectrum. The regeneration of $\nu_\tau$ is found to have an insignificant effect on the conversion of $\nu_\tau$ to air shower, a contribution of less than 2%. Cerenkov light may dominate over fluorescence light and become the main light source to trigger the CRTNT detectors. An air shower development algorithm has been developed using Corsika in a uniform atmosphere for estimating trigger efficiency. Fluorescence/Cerenkov light production and propagation are fully simulated. Detector response is also fully simulated. The detector configuration is optimized using this simulation tool. The CRTNT detector simulation indicates that a rate of about eight events per year for an optimized detector with 15% duty cycle is expected for the AGN source model [12].

With such a sensitivity and an estimated angular resolution better than $2^\circ$, the CRTNT detector can be used to search for nearby cosmic ray sources, e.g. our galactic centre (GC). Since gamma rays are blocked by dust near the GC and cosmic rays are bent away from the GC due to the strong magnetic field around the GC, the neutrino is a unique particle for exploring the GC region. At the site near Mt Wheeler Peak, the GC rises above the horizon during summer nights and reaches its highest elevation at about $20^\circ$. The GC would be well covered by the CRTNT detector if the detectors face south. Therefore, to balance between the use of the mountain as a converter and the duration during which the GC can be seen, we turn all the telescopes about $30^\circ$ to the south. The field of view of the reconfigured CRTNT detector is shown in figure 3 by the dashed lines. The neutrino event trigger efficiency would remain essentially unchanged. However, about a 1000 h exposure of the GC could be expected during a 3 year run.

## Acknowledgments

MAH and ZC are grateful to G L Lin and J J Tseng for theoretical support. Many thanks from ZC to R W Springer for very fruitful discussions. This work (ZC) is partially supported by the Key Laboratory of Particle Astrophysics China, by Innovation fund (U-526) of IHEP, China and by Hundred Talents & Outstanding Young Scientists Abroad Program (U-610) of IHEP, China. ZC and PS are partially supported by US NSF grants PHY 9974537 and PHY 9904048, while MAH is supported by Taiwan NSC grant 92-2119-M-239-001.

## References

[1] Fukuda Y *et al* (Super-Kamiokande Collaboration) 1998 *Phys. Rev. Lett.* **81** 1562
Fukuda Y *et al* (Super-Kamiokande Collaboration) 1999 *Phys. Rev. Lett.* **82** 1810
Fukuda Y *et al* (Super-Kamiokande Collaboration) 2000 *Phys. Rev. Lett.* **85** 3999
[2] Athar H, Jezabek M and Yasuda O 2000 *Phys. Rev.* D **62** 103007
Beacom J F, Crotty P and Kolb E W 2002 *Phys. Rev.* D **66** 021302(R)
[3] Feng J L *et al* 2002 *Phys. Rev. Lett.* **88** 161102 and references therein
[4] Fargion D 2002 *Astrophys. J.* **570** 909
[5] Hou G W S and Huang M A 2002 *Proc. First NCTS Workshop on Astroparticle Physics (Kenting, Taiwan)* ed H Athar, G L Lin and K N Ng (Singapore: World Scientific) p 105 (*Preprint* astro-ph/0204145)
[6] Huang M A, Tseng J J and Lin G L 2003 *Proc. 28th ICRC (Tsukuba, Japan)* p 1427
[7] Gandhi R *et al* 1999 *Phys. Rev.* D **58** 093009
[8] Dutta S I *et al* 2001 *Phys. Rev.* D **63** 094020
[9] Tseng J J *et al* 2003 *Phys. Rev.* D **68** 063003
[10] Abu-Zayyad T *et al* 2001 *Astrophys. J.* **557** 686
[11] Swordy S P and Kieda D B 2000 *Astropart. Phys.* **13** 137
[12] Semikoz D and Sigl G 2004 *J. Cosmol. Astropart. Phys.* JCAP04(2004)3
[13] Waxman A and Bahcall J 1997 *Phys. Rev. Lett.* **78** 2292
[14] Sigl G *et al* 1998 *Phys. Rev.* D **59** 043504
[15] Yoshida S, Sigl G and Lee S 1998 *Phys. Rev. Lett.* **81** 5055
[16] Stecker F W *et al* 1991 *Phys. Rev. Lett.* **66** 2697
[17] Heck D *et al* 1998 *Preprint FZKA-6019* Institut fur Kernphys., University of Karlsruhe
[18] Nagano M *et al* 2004 New measurement on photon yields from air and the application to the energy estimation of primary cosmic rays (*Preprint* astro-ph/0406474)
[19] Abu-Zayyad T *et al* 2001 *Astrophys. J.* **557** 686
[20] Abbasi R U *et al* 2004 Techniques for measuring atmospheric aerosols for air fluorescence experiments *Astropart. Phys.* submitted
[21] Stecker B W and Salamon M H 1996 *Space Sci. Rev.* **75** 341
[22] Hill G C (For the AMANDA Collaboration) 2001 *Proc. 36th Recontres de Moriond, Electroweak Interactions and Unified Theories (March 2001)* (*Preprint* astro-ph/0106064)